Brief Communication

MOLECULAR METABOLISM

WWOX somatic ablation in skeletal muscles alters glucose metabolism

Muhannad Abu-Remaileh [1], Monther Abu-Remaileh [2], Rania Akkawi [1], Ibrahim Knani [3], Shiran Udi [3], Micheal E. Pacold [4], Joseph Tam [3], Rami I. Aqeilan [1,5,*]

ABSTRACT

Objective: *WWOX*, a well-established tumor suppressor, is frequently lost in cancer and plays important roles in DNA damage response and cellular metabolism.

Methods: We re-analyzed several genome-wide association studies (GWAS) using the *Type 2 Diabetes Knowledge Portal* website to uncover WWOX's association with metabolic syndrome (MetS). Using several engineered mouse models, we studied the effect of somatic WWOX loss on glucose homeostasis.

Results: Several *WWOX* variants were found to be strongly associated with MetS disorders. In mouse models, somatic ablation of *Wwox* in skeletal muscle ($Wwox^{\Delta SKM}$) results in weight gain, glucose intolerance, and insulin resistance. Furthermore, $Wwox^{\Delta SKM}$ mice display reduced amounts of slow-twitch fibers, decreased mitochondrial quantity and activity, and lower glucose oxidation levels. Mechanistically, we found that WWOX physically interacts with the cellular energy sensor AMP-activated protein kinase (AMPK) and that its loss is associated with impaired activation of AMPK, and with significant accumulation of the hypoxia inducible factor 1 alpha (HIF1α) in SKM.

Conclusions: Our studies uncover an unforeseen role of the tumor suppressor WWOX in whole-body glucose homeostasis and highlight the intimate relationship between cancer progression and metabolic disorders, particularly obesity and type-2 diabetes.

Subject areas: Genetics, Metabolic Syndrome, Diabetes.

Keywords Metabolic syndrome; Tumor suppressor; T2D; WWOX; AMPK

1. INTRODUCTION

Metabolic syndrome (MetS) is a major health problem, with an average worldwide prevalence of 25% among adults [1]. MetS encompasses a cluster of disorders including obesity, high blood pressure, and high fasting glucose levels that are caused by insulin resistance in peripheral tissues, mainly in skeletal muscles (SKM) and liver [2]. MetS is associated with fatal cardiovascular diseases and the development of type-2 diabetes mellitus (T2D) [2].

Comprising 40%–50% of the body mass, SKM represent the largest body organ. SKM are responsible for 85% of all insulin-mediated glucose clearance [3], highlighting their importance in maintaining whole-body glucose homeostasis [4]. SKM are composed of two types of fibers: oxidative slow-twitch fibers and glycolytic fast-twitch fibers, although muscle fibers are flexible and can transform from one state into another in response to energetic demands [5]. Notably, the SKM of T2D and obese patients have been shown to display a decreased oxidative capacity [6], by transitioning from oxidative slow-twitch muscle fibers into glycolytic fast-twitch fibers [7]. The factors that regulate this transition and its dynamics might modulate cellular metabolism, whereas their perturbations could lead to the development of metabolic disorders.

WWOX is a tumor suppressor that is commonly lost in several human malignancies [8]; its overexpression inhibits tumor growth and enhances apoptosis [9,10]. *WWOX* encodes a 46 kDa protein that contains two N-terminal WW domains, known to mediate protein–protein interactions, and a central short-chain dehydrogenase/reductase (SDR) domain [10], whose function is still unknown. WWOX pleotropic tumor suppressor functions include promoting apoptosis and DNA repair and antagonizing aerobic glycolysis [11].

Several reports have implicated WWOX function in cellular metabolism [12–14]. In a previous work, we showed that WWOX regulates glucose metabolism in tissue culture cells via suppressing hypoxia-inducible factor 1-alpha (HIF1α) [15]. WWOX physically interacts with HIF1α and suppresses its activity, leading to activation of oxidative phosphorylation (OXPHOS) and inhibition of glycolysis to maintain a balanced cellular glucose metabolism [16]. *Wwox* null mice die by the age of 3 weeks due to severe hypoglycemia [17],

[1]The Lautenberg Center for General and Tumor Immunology, Department of Immunology and Cancer Research-IMRIC, Hebrew University-Hadassah Medical School, Jerusalem, Israel [2]Whitehead Institute for Biomedical Research, 9 Cambridge Center, Cambridge, MA 02142, USA [3]Obesity and Metabolism Laboratory, The Institute for Drug Research, School of Pharmacy, Faculty of Medicine, The Hebrew University of Jerusalem, Jerusalem 9112001, Israel [4]Department of Radiation Oncology, New York University Langone Medical Center, 522 First Avenue, Smilow 907, New York, NY, USA [5]Department of Cancer Biology and Genetics, Wexner Medical Center, The Ohio State University, Columbus, OH, USA

*Corresponding author. Lautenberg Center for Immunology and Cancer Research, Hebrew University-Hadassah Medical School, PO Box 12272, Ein Karem Campus, Jerusalem 91120, Israel. E-mail: ramiaq@mail.huji.ac.il (R.I. Aqeilan).

Received December 9, 2018 • Revision received January 18, 2019 • Accepted January 25, 2019 • Available online 31 January 2019

https://doi.org/10.1016/j.molmet.2019.01.010

hence precluding the study of WWOX physiological functions in adult mice. To overcome this issue, a conditional knockout mouse model in which *Wwox* can be deleted in a time- and tissue-specific manner was recently generated [18]. Using this novel model, we recently showed that WWOX somatic ablation in mammary epithelium is associated with mammary tumor formation and p53 impaired function [19]. Moreover, specific WWOX deletion in hepatocytes accelerates the development of hepatocellular carcinoma (HCC), partly due to the promotion of HIF1α activity [20].

In this report, we screened for the metabolic function of WWOX using engineered mouse models in which the murine *Wwox* gene was specifically deleted in the main metabolic peripheral organs including liver, adipose tissue, and SKM. Interestingly, we found that only mice with SKM-specific ablation of *Wwox* develop a phenotype resembling MetS, as manifested by hyperglycemia, obesity, and dyslipidemia. Remarkably, *Wwox* ablation in SKM is associated with decreased carbohydrate oxidation, fewer slow-twitch muscle fibers, and reduced mitochondrial mass. Mechanistically, WWOX loss is associated with impaired HIF1α and AMPK activity.

2. RESULTS

2.1. The *WWOX* gene is frequently altered in MetS

Genome-wide association studies (GWAS) have linked several single nucleotide polymorphisms (SNPs) in *WWOX* with obesity [21,22] and T2D [23,24]. To systematically study the role of WWOX in MetS, we reanalyzed GWAS datasets (n = 27) from the *Type 2 Diabetes Knowledge Portal* website (www.type2diabetesgenetics.org). Several *WWOX* variants were found to be strongly associated with MetS disorders including T2D (Figure S1A), high fasting glucose (Figure S1B), abnormal waist circumference (Figure S1C), high body mass index (BMI; Figure S1D), and dysregulated triglyceride levels (Figure S1E). Notably, several of these variants lie in the *WWOX* coding sequence and some are predicted to change its amino acid sequence (Supplementary Table 1). These data provide genetic evidence for the involvement of WWOX in MetS disorders.

2.2. Conditional ablation of murine *Wwox* in peripheral metabolic tissues

To investigate the role of WWOX in metabolic homeostasis, we conditionally deleted its gene in the main peripheral metabolic tissues: the liver, adipose tissue, and SKM (Figure 1A). To this end, the *Wwox*-floxed mouse ($Wwox^{f/f}$) [18] was bred with either *Albumin-Cre* [25], *Adiponectine-Cre* [26], or *ACTA1-rtTAtetO-Cre* [27] to delete the *Wwox* gene specifically in hepatocytes (Figure 1B), adipocytes (Figure 1C), or SKMs (Figure 1D), respectively. Thereafter, we tested the effects of WWOX loss on whole-body metabolism by monitoring fasting blood glucose levels and body weight. Although WWOX loss in hepatocytes and adipocytes had no significant effects on fasting glucose levels compared with their control littermate mice (*Cre+, Wwox+/+),* a significant increase was observed in mice with muscle-specific ablation of *Wwox* ($Wwox^{\Delta SKM}$) (Figure 1E). Likewise, only mice that lost WWOX in the muscle were defective in their ability to clear glucose, as determined by the glucose tolerance test (GTT) (Figure 1F—H). Finally, $Wwox^{\Delta SKM}$ mice gained significantly more weight than their wild type controls (Figure 1K), with no similar trend observed in mice lacking the *Wwox* gene in the liver or adipocytes (Figure 1I and J). These data indicate that WWOX expression in SKM is essential for organismal glucose homeostasis.

2.3. *Wwox*-specific ablation in skeletal muscles is associated with insulin resistance

To better understand the role of WWOX in SKM and its contribution to metabolic homeostasis, we further characterized the $Wwox^{\Delta SKM}$ mice. Although no major differences were observed in SKM histology (Figure 2A), an analysis of their body composition revealed a significant increase in the fat content with a concomitant decrease in the lean body component (Figure 2B). Moreover, $Wwox^{\Delta SKM}$ mice exhibited a decreased HDL/LDL ratio as well as high levels of triglycerides and cholesterol, compared with control littermates (Figure 2C and D), suggesting that $Wwox^{\Delta SKM}$ mice are predisposed to MetS.

Insulin resistance is a hallmark of metabolic deregulation and is tightly associated with MetS. Indeed, we found that, unlike control mice or mice lacking WWOX expression in the liver or adipocytes, $Wwox^{\Delta SKM}$ mice suffer from insulin resistance (Figure 2E—G), and consequently, their basal insulin levels after fasting are much higher (Figure 2H). To further confirm these observations, we performed an *in-vivo* glucose uptake assay using radioactive (^{18}F)-FDG and a PET-CT scan. We found that $Wwox^{\Delta SKM}$ mice uptake less glucose into gastrocnemius (Figure 2I) and hamstring muscles (Figure 2J); however, their glucose uptake in the brain or the liver is not affected (Figure 2SA and B). These data suggest an autonomous defect in glucose uptake in SKM in the absence of WWOX.

2.4. *Wwox*-specific ablation in skeletal muscles is associated with metabolic reprograming

In order to assess the metabolic and physical activity of $Wwox^{\Delta SKM}$ mice, we next monitored these mice using metabolic cages, as previously described [28]. $Wwox^{\Delta SKM}$ mice exhibited decreased respiratory quotient (RQ) compared with control mice, in particular, during the active dark period of the day cycle (Figure 3A and B). Interestingly, $Wwox^{\Delta SKM}$ mice displayed increased fat oxidation (Figure 3C and D), whereas carbohydrate oxidation decreased (Figure 3E and F). Although these mice gained body weight as a function of age (Figure 1K), the amount of food intake during the dark active period was decreased, compared with control mice (Figure 3G and H). Importantly, $Wwox^{\Delta SKM}$ mice exhibited no difference in activity neither in the active dark period nor in the daylight period (Figure 3S A—H). Hence, the reduced locomotor activity can be excluded as a cause for fat storage, suggesting a metabolic rewiring at the organismal level.

In accordance with these findings, $Wwox^{\Delta SKM}$ mice exhibited decreased mitochondrial-OXPHOS-dependent slow-twitch fibers, with no change in the glycolytic fast-twitch-dependent fibers (Figure 3I), as determined by the measurement of myosin and troponins mRNA expression [29]. Interestingly, we found that WWOX levels are higher in the slow-twitch soleus fibers, compared with the fast-twitch extensor digitorum longus (EDL) fibers in *Wwox* wild-type muscle (Figure 4S). These findings were also consistent with the decreased mitochondrial mass and Krebs cycle gene levels in the SKMs of $Wwox^{\Delta SKM}$ (Figure 3J and K). Taken together, our data suggest a defect in mitochondrial oxidation. Indeed, serum lactate levels were significantly elevated in $Wwox^{\Delta SKM}$ mice (Figure 3L). Likewise, we also observed an upregulation of lactate production (LDHA1) and exportation genes (MCT4), coupled with elevation of other HIF1α-regulated glycolytic genes (Figure 3M). Thus, our findings indicate that *Wwox* ablation in SKM disrupts the intra-muscular energetic balance by suppressing mitochondrial glucose oxidation and activating lactate production, leading to disruption of whole-body glucose homeostasis and development of MetS.

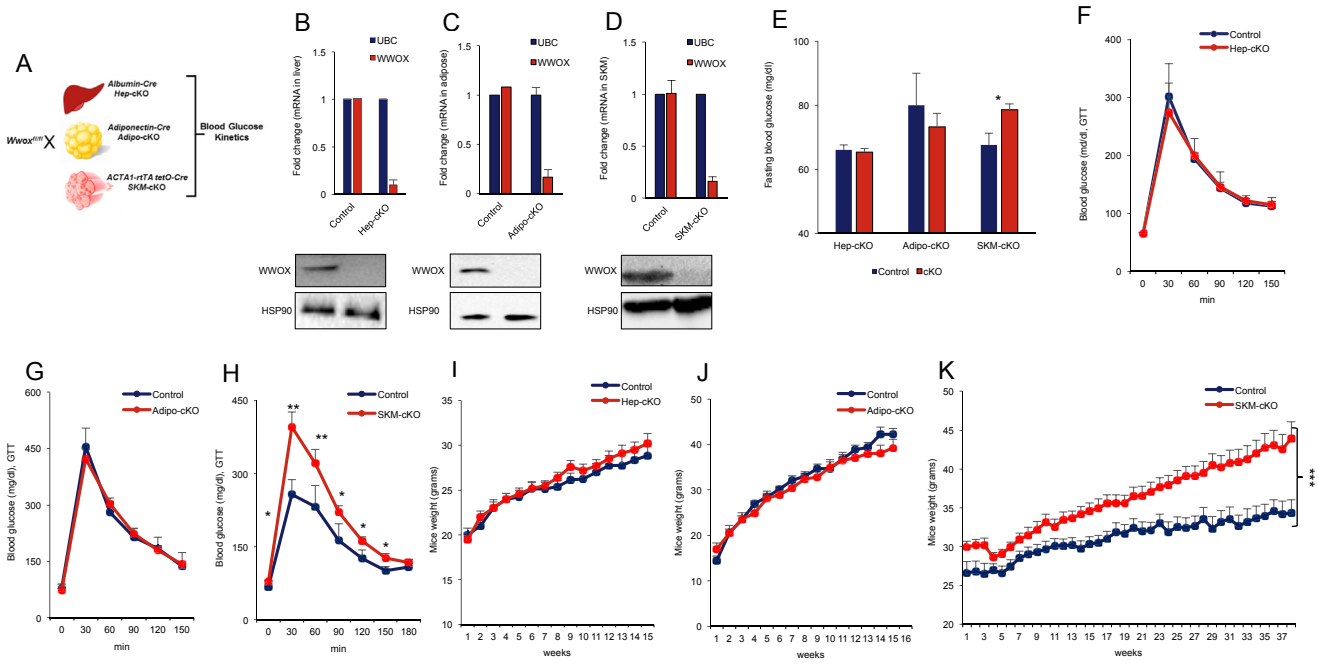

Figure 1: Glucose homeostasis in *Wwox* conditional mouse models. (A) Work plan and animal model used in the study. *Wwoxf/f* genetically engineered mice were crossed with *Albumin-Cre* mice in order to delete *Wwox* specifically in hepatocytes (*Hep-cKO*) or *Adiponectin-Cre* mice in order to delete *Wwox* specifically in adipocytes (*Adipo-cKO*) or with *ACTA1-etTA tetO-Cre* transgenic mice in order to delete *Wwox* specifically in skeletal muscles (*SKM-cKO*). Validation of WWOX deletion in livers of *Hep-cKO* (B), in adipose tissue of *Adipo-cKO* (C), and in skeletal muscles *SKM-cKO* (D) using qRT-PCR and immunoblotting; n = 3 for each mouse group. (E) Blood glucose level (mg/dl) measured after 18 h of overnight fasting in control mice versus *Hep-cKO, Adipo-cKO,* or *SKM-cKO* mice; n = 8 of each group. Glucose tolerance test (GTT) was used for control mice versus *Hep-cKO* (F), *Adipo-cKO* (G), or *SKM-cKO* (H) mice at 6 months of age for all groups. Mice were injected with 2g/Kg glucose at zero time after 18 h overnight fasting and serum glucose was measured for up to 2.5 h; n = 8 for each group. Total body weight was measured in grams once a week for control mice versus *Hep-cKO* (I), *Adipo-cKO* (J), or *SKM-cKO* (K). The Y-axis represents the number of follow-up weeks. Mice weighing started at the age of 6–8 weeks; n = 8 for each group. * indicates P-value <0.05, ** P-value <0.01, *** P-value <0.001. Error bars indicate ± SEM. cKO: conditional knockout. Control mice in all analysis have Cre expression in *Wwox*+/+ background (Alb-Cre+;*Wwox*+/+, *Adipo-Cre*+;*Wwox*+/+, *ACTA1-etTA tetO-Cre*+;*Wwox*+/+, respectively).

2.5. WWOX regulates central metabolic proteins in skeletal muscles

In order to better understand how WWOX regulates the metabolic state in skeletal muscles, we tested the effects of its loss on a number of key metabolic pathways. We have previously shown that WWOX modulates HIF1α by inhibiting its accumulation and function under normoxic conditions [15]. We therefore set out to examine whether HIF1α levels and function are enhanced in $Wwox^{\Delta SKM}$ mice. Indeed, we found elevated HIF1α protein levels in quadriceps muscles of $Wwox^{\Delta SKM}$ mice (Figure 4A and B). Moreover, the levels of *Pkm2* and *Pdk1*, key glycolytic genes, regulated by HIF1α, were also elevated in SKM of these mice (Figure 4A and B), indicating that HIF1α is functionally active in *Wwox*-deficient skeletal muscles, consistent with previous observations in *Wwox*-null mice (Abu-Remaileh and Aqeilan, 2014).

Another key player in glucose homeostasis and cellular metabolism is AMPK, which has been reported to be inactivated in MetS disorders [30], and its reactivation has been recently suggested as a new therapeutic approach to MetS [31]. Hence, we examined AMPK activation and found that Thr172 phosphorylation of AMPK (p-AMPK) is completely disrupted in skeletal muscles of $Wwox^{\Delta SKM}$ mice (Figure 4A and B). Notably, the phosphorylated form of acetyl-CoA carboxylase (p-ACC), a canonical substrate of AMPK, was also decreased, indicating an AMPK decreased activity upon *Wwox*-specific deletion in SKM (Figure 4A and B). Interestingly, fat tissues of $Wwox^{\Delta SKM}$ mice display no major changes in the previously mentioned metabolic proteins (Figure 5S). These results suggest that WWOX could act as a positive regulator of AMPK activity in SKM.

To address whether WWOX regulates AMPK activation, we transfected the mouse myoblast C2C12 cell line with siRNA against murine *Wwox* and tested AMPK levels and activity. As seen in Figure 4C and D, p-AMPK is decreased upon acute WWOX depletion, consistent with a possible role of WWOX in directly regulating AMPK activation.

To further delineate this crosstalk, we investigated whether WWOX, a known adaptor protein, is physically associated with AMPK protein. To this end, HEK293T cells, which can be transfected easily and are frequently used in our lab to check WWOX interactome [32], were co-transfected with Flag-AMPK1α and HA-WWOX, followed by immunoprecipitation with anti-Flag or anti-HA, or anti-IgG as a negative control. We indeed found that both exogenous proteins interact with each other (Figure 4E). Moreover, we detected specific endogenous WWOX and p-AMPK protein interaction in C2C12 muscle cells (Figure 4F), implying functional crosstalk between the two metabolic proteins. Taken together, these results indicate that WWOX deletion in SKM leads to a failure in proper AMPK activation, and an enhanced activation of HIF1α, leading to disruption of metabolic balance in SKM and the development of MetS disorders (Figure 4G).

3. DISCUSSION

SKM is a fundamental peripheral tissue that is involved in glucose homeostasis. Impaired glucose uptake and insulin resistance in SKM is a major cause of T2D and other metabolic disorders [33]. In fact, a disruption in OXPHOS, mitochondrial activity, fatty acid oxidation, and glycolysis in SKM is suggested as the main cause of failure of glucose

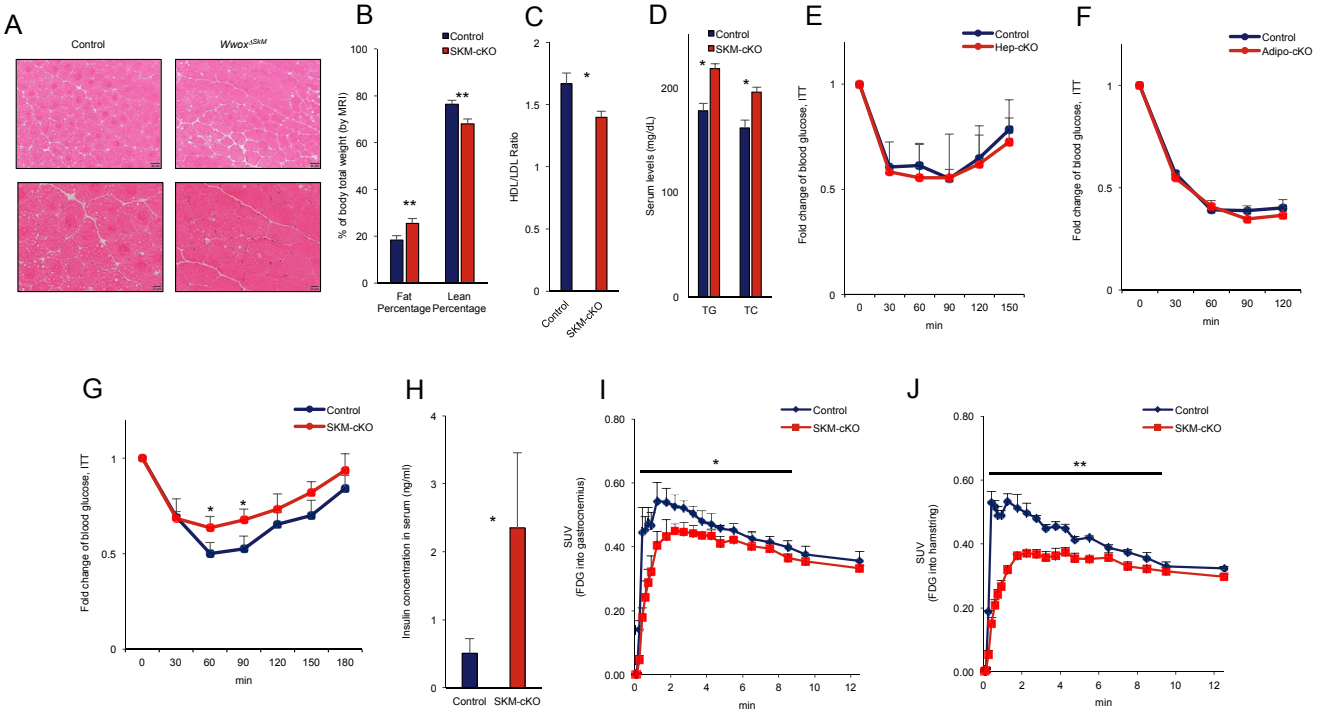

Figure 2: *Wwox*-specific ablation in skeletal muscles leads to insulin resistance. (A) H&E staining for quadriceps cross-sections of control and *Wwox SKM-cKO* mice (the upper image bar is 50 μm, the lower image bar is 20 μm). (B) Fat and lean percentage from the total body weight of control mice and *Wwox SKM-cKO* mice measured by MRI. (C) and (D) Serum HDL/LDL ratio. Triglycerides (TG) and total cholesterol (TC) of control mice and *Wwox SKM-cKO* mice were measured by Cobas analyzer. (I) Insulin tolerance test (ITT) for 10-month-old mice. Control and *Hep-cKO* (E), or *Adipo-cKO* (F), or *SKM-cKO* (G) mice were injected with 0.75 U/kg insulin at time zero followed by 4 h fasting and serum glucose was measured for up to 3 h. (H) Serum insulin levels of control and *Wwox SKM-cKO* mice (control n = 4; SKM-cKO n = 4) measured by ELISA. Glucose uptake assessment into gastrocnemius (I) and hamstring (J) skeletal muscles were assessed by PET-CT scan. * indicates P-value <0.05, ** P-value <0.01, *** P-value <0.001. Error bars indicate ± SEM. All assays were done on control mice n = 8; SKM-cKO mice n = 9.

homeostasis [34]. Therefore, identifying the main regulators of SKM glucose metabolism is of great interest.

Over the last decade, many GWAS studies have reported several genetic variants in *WWOX* as among the most significant SNPs and variants associated with obesity and T2D [22,24]. However, a direct role of WWOX involvement in metabolic disorders is unclear. Here, we demonstrated a novel function for the tumor suppressor WWOX in SKM metabolism. We found that specific ablation of murine *Wwox* in SKM could lead to obesity, hyperglycemia, and insulin resistance. These metabolic abnormalities were associated with decreased mitochondrial mass and reduced OXPHOS, hence impairing the bioenergetic balance. At the molecular level, our findings reveal an important functional crosstalk between WWOX and HIF1α, as well as between WWOX and AMPK in SKM. These observations may suggest that germline mutations in the *WWOX* gene result in impaired glucose homeostasis as a result of SKM metabolic dysfunction.

MetS and impaired glucose homeostasis are commonly caused by defects in peripheral organs involved in glucose uptake and utilization including liver, adipose tissue, and SKM. Characterizing the metabolic phenotypes of different mouse models that harbor *Wwox* deletion in each of these organs revealed that only WWOX's loss of function in SKM is associated with phenotypes resembling MetS. Although WWOX inactivation in liver and adipocytes did not reveal a defect in glucose homeostasis and body weight regulation, this does not exclude a function of WWOX in other metabolic pathways or nutrient states, which were not addressed in this study. In fact, specific deletion of *Wwox* in hepatocytes was shown to be associated with impaired lipid metabolism [13], consistent with the susceptibility of certain WWOX variants to cardiovascular diseases [13]. More recently, we demonstrated that WWOX ablation in hepatocytes is associated with acceleration of HCC development due to enhanced proliferation mediated by a glycolytic switch [20].

The phenotypes observed upon WWOX ablation in SKM were very prominent. Increased body weights, fat-to-lean ratios, and circulating fats were evident in $Wwox^{\Delta SKM}$ mice. Moreover, these mice displayed impaired GTT and ITT, and manifested hyperglycemia and hyperinsulinemia, indicating a state of insulin resistance. Furthermore, an *in-vivo* ^{18}F-FDG glucose uptake assay demonstrated a specific decrease in SKM glucose uptake. Although these mice developed hyperglycemia, they mainly relied on fatty oxidation as a main source of cellular energy. Consistent with these findings, we observed a decrease in the quantity of oxidative-dependent slow-twitch fibers in SKM of $Wwox^{\Delta SKM}$ mice. These observations are consistent with differential WWOX function in soleus slow-twitch muscles, expressing relatively higher levels of WWOX, when compared to EDL fast-twitch muscles. Moreover, decreased mitochondrial mass suggests inhibition of OXPHOS and carbohydrate oxidation. In accordance, the levels of lactate serum, the lactate exporter MCT4, and the lactate dehydrogenase enzyme LDHA1 were all found to be elevated in $Wwox^{\Delta SKM}$ mice, indicating enhanced glycolysis. In general, these metabolic perturbations mimic the metabolic status of hyperglycemic T2D human patients [35]. In fact, the SKM of T2D human patients present a downregulated mitochondrial OXPHOS and decreased mitochondrial DNA content [36,37]. Furthermore, T2D patients exhibit an increased rate of glycolysis and lactate production [38], further suggesting high similarities between human T2D patients and *Wwox* deletion in SKM.

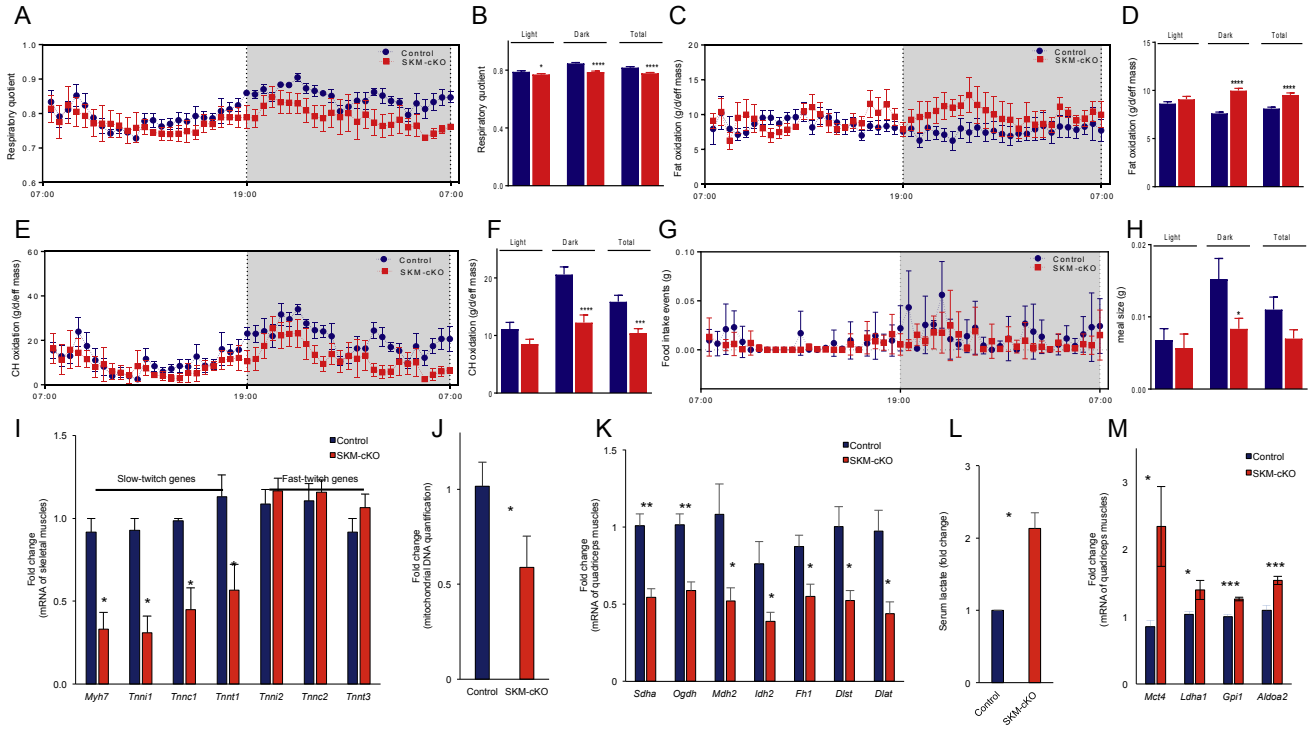

Figure 3: *Wwox*-specific ablation in skeletal muscles is associated with decreased glucose oxidation. A–H: Metabolic cage analysis of control and *Wwox SKM-cKO* mice was measured every 0.5hr for 24hr (48 measurements); (n = 8 for each group). Respiratory quotient (RQ) chart (A), total RQ (B), fat oxidation (g/d/eff mass) chart (C), total fat oxidation (D), carbohydrate oxidation (CHO) chart (E), total CHO (F), food intake events chart (G), and total food intake (H). (I) mRNA levels of slow-twitch myosin *Myh7*, *Tnni1*, *Tnnc1,* and *Tnnt1* vs fast-twitch troponin genes *Tnni2*, *Tnnc2,* and *Tnnt3* in muscles of control and *Wwox SKM-cKO* mice quantified by qRT-PCR (n = 4 for each group). (J) Quantification of mitochondrial DNA in skeletal muscles of control and *Wwox SKM-cKO* mice as assessed by qRT-PCR (n = 4 for each group). (K) mRNA levels of Krebs cycle genes; *Sdha*, *Ogdh*, *Mdh2*, *Idh2*, *Fh1*, *Ddlst,* and *Dlat* in quadriceps of control and *Wwox SKM-cKO* mice quantified by qRT-PCR (n = 4 for each group). (L) Serum lactate fold change of control and *Wwox SKM-cKO* mice as assessed by MSPEC (n = 6 for each group). (M) mRNA levels of lactate transporter *Mct4* and glycolytic HIF1α target genes; *Ldha1*, *Gpi1,* and *Aldoa2* in quadriceps of control and *Wwox SKM-cKO* mice quantified by qRT-PCR (n = 4 for each group).

These data imply that WWOX in SKM plays a central role in regulating glucose catabolic pathways and antagonizes the development of the MetS.

Although $Wwox^{\Delta SKM}$ mice weighed more, a snapshot analysis of their 24-hour food consumption revealed that these mice eat less during their dark active period. These results might be explained by the high systemic insulinemia, which is known to affect central pathways that modulate feeding [39], as well as play a lipogenic role in adipose tissue [40], suggesting that MetS and insulin resistance have a SKM cell-autonomous effect.

At the molecular level, WWOX is known to play pleotropic roles in different contexts including DNA damage response and cellular metabolism [11]. In our current study, we demonstrate that WWOX loss could lead to significant changes in two main pathways: HIF1α and AMPK. Consistent with previous observations [15], we show that upon WWOX loss, HIF1α levels are elevated in SKM of $Wwox^{\Delta SKM}$ mice. This elevation in HIF1α levels was accompanied by increased trans-activation activity of the main glycolytic genes, resulting in their upregulation. Although the increased glycolysis does not seem massive, still, upregulated PDK1 levels blocked glucose influx into the Krebs cycle, leading to decreased glucose oxidation. Moreover, HIF1α was reported to inhibit Krebs cycle genes and mitochondrial mass [41,42], which is in accordance with the phenotype observed in $Wwox^{\Delta SKM}$ mice.

AMPK is a serine/threonine kinase sensor that is activated upon a drop of the energy status in the cell, namely, by elevated levels of AMP [43]. Once phosphorylated (activated), AMPK phosphorylates a number of target proteins and alters their functions, resulting, for example, in inhibition of lipid metabolism and activation of fatty acid oxidation through ACC1 and ACC2 [44]. Upon WWOX loss, AMPK activation is hampered in SKM of $Wwox^{\Delta SKM}$ mice, as revealed by its decreased phosphorylation on residue T-172. AMPK activation increases fatty acid oxidation in SKM [45]. The increased systemic fat oxidation in $Wwox^{\Delta SKM}$ mice, as assessed by metabolic cages, may be explained as a compensatory effect for impaired catabolic pathways of carbohydrate oxidation. Moreover, the inhibition of ACC2 in SKM by phosphorylation, known to enhance fatty acid oxidation in SKM [46], is indeed impaired and may explain the decreased glucose oxidation and increased fatty acid oxidation in $Wwox^{\Delta SKM}$ mice, which is also demonstrated by knocking down *Wwox* in C2C12 muscle cells. Since AMPK is an activator of mitochondrial respiration [47] and inhibits lipogenesis through inhibition of ACC [48], WWOX loss could result in improper activation of AMPK and hence decreased OXPHOS. This could affect many metabolic pathways in other active metabolic organs, such as adipose tissue and liver, to increase their dependence on fatty acid oxidation [49].

We propose that WWOX regulates the proper activation of AMPK in order to respond to nutrient stress conditions and maintain the homeostasis of the skeletal muscles. Under normal physiological conditions, AMPK is mostly inactive; however, under stress (for example, starvation), WWOX protein levels are elevated, leading to enhanced activation of AMPK. Therefore, it is reasonable to assume

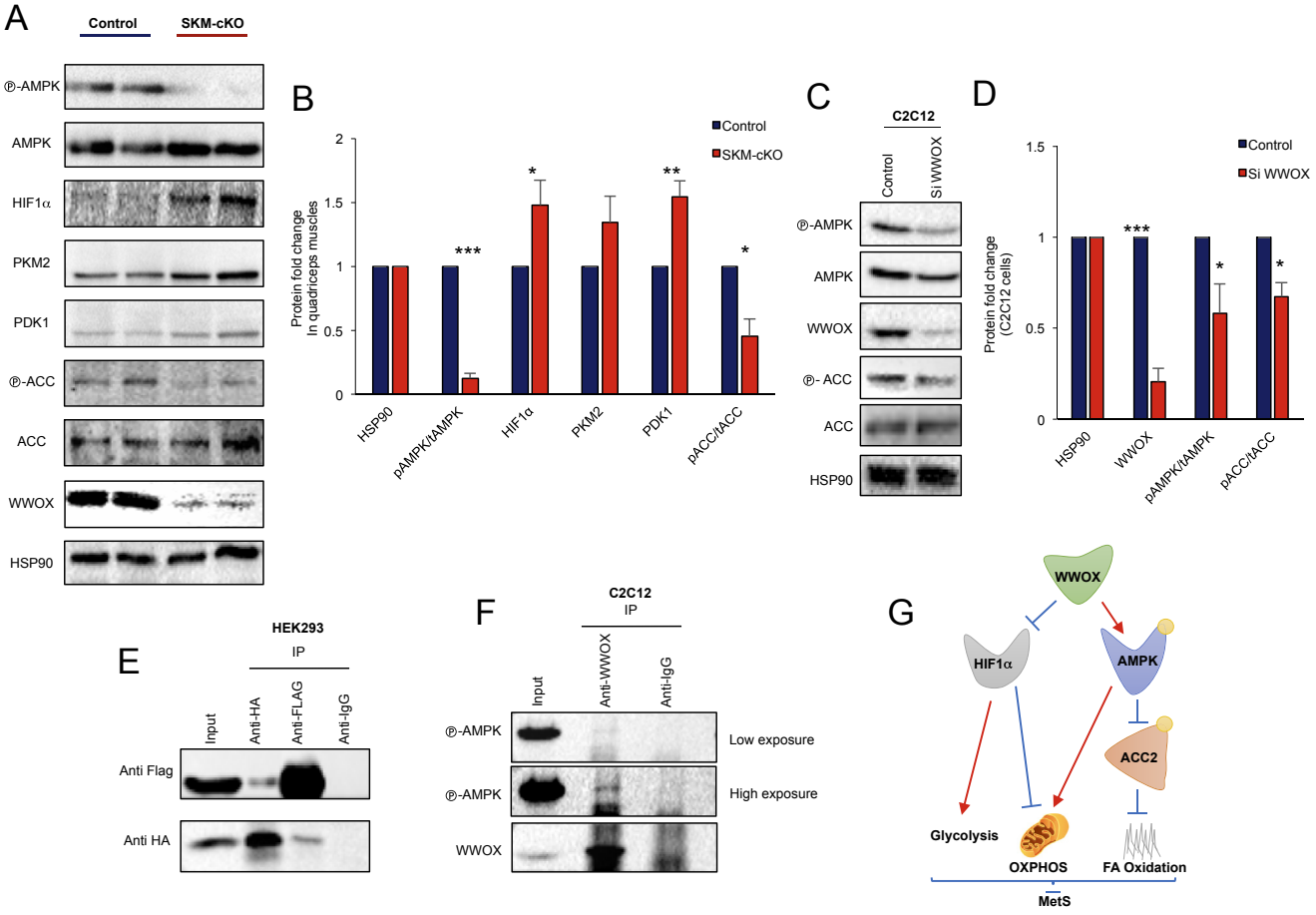

Figure 4: WWOX regulates central metabolic proteins in skeletal muscles. (A) Immunoblotting of HIF1α, PKM2, PDK1, pAMPK, total-AMPK, pACC, total-ACC, and WWOX protein levels in quadriceps of control and *Wwox*-SKM-cKO mice. Representative blots of two mice for each group is shown. (B) Quantification of the pAMPK/tAMPK ratio, the HIF1α, PKM2, PDK1, and pACC/tACC ratio of 3 different control and SKM-cKO mice presented as fold change. (C) pAMPK levels in C2C12 cells after WWOX knockdown using siRNA. (D) Quantification of the pAMPK/tAMPK ratio, the WWOX and pACC/tACC ratio of control and si-WWOX-transfected cell lines presented as the fold change. (E) Co-immunoprecipitation experiments showing physical interaction between WWOX and AMPK. Flag-AMPK and HA-WWOX were co-transfected in HEK293T cells. Lysates were immunoprecipitated with anti-HA or anti-FLAG, followed by immunoblotting with the indicated antibodies. Anti-IgG was used as a negative control. (F) Immunoprecipitation experiment showing physical interaction between endogenous WWOX and pAMPK in C2C12 muscle cells. Lysates were immunoprecipitated with mouse monoclonal anti-WWOX or anti-IgG, followed by immunoblotting with polyclonal anti-WWOX or anti-pAMPK. Low and high exposure blots for WWOX antibody are shown. (G) A model showing WWOX inhibition of HIF1α and proper activation of AMPK, resulting in enhanced mitochondrial function and antagonizing of MetS. Band quantification of western blots was done by the ImageJ program. * indicates P-value <0.05, ** P-value <0.01, *** P-value <0.001. Error bars indicate ± SEM. Protein levels were quantified from control mice n = 3; SKM-cKO mice n = 3 or control cell lines n = 4; treated cell lines n = 4. Representative blots are shown.

that elevated levels of WWOX mimic the poor energetic status of the cells, resulting in AMPK activation and hence, increased glucose oxidation. Under normal conditions, we failed to observe an AMPK activation in WWOX-depleted cells, suggesting that WWOX is required for this important cellular response. In fact, we found that WWOX knockdown resulted in impaired activation of AMPK, suggesting that WWOX is most likely an upstream regulator of AMPK. Furthermore, we provided evidence that WWOX physically binds AMPK, indicating a functional interaction between these two proteins. Therefore, it is possible that WWOX deficiency signals a state of excess nutrients and thus AMPK is not activated, leading to the accumulation of extracellular glucose and hyperglycemia. Further studies will be necessary to examine the functional association between WWOX and AMPK.

By analyzing human data sets in the T2D portal, we revealed a significant association between WWOX variants and a number of metabolic disorders including T2D, obesity, BMI, and many others. Interestingly, several of these variants are located in the *WWOX* coding region, and they are expected to generate mutations in WWOX protein. Future studies should investigate the effect of these variants on WWOX protein function and stability, as well as how they modulate AMPK and HIF1α functions.

Although it has been reported that AMPK is a critical modulator of HIF1α transcriptional activity in hypoxic DU145 prostate cancer cells [50], very little is known about the cross-talk between AMPK and HIF1α in SKM [51]. Our results, presented here, provide, for the first time, clear evidence that WWOX plays a key role in glucose homeostasis in SKM by regulating AMPK and HIF1α. WWOX maintains a proper AMPK activation and restricts HIF1α activity, resulting in balanced glucose metabolism circuits in SKMs. Upon WWOX deficiency, AMPK activation becomes dysfunctional and HIF1α accumulates, leading to reduced mitochondrial oxidation, augmented glycolysis, and fatty acid oxidation, which can lead to the development of MetS (Figure 4G).

4. METHODS

4.1. Animal models

Wwox-floxed (*Wwoxfl/fl*) C57BL6/J; 129sv mixed genetic background mice [18] were crossed with the following transgenic mice: *Albumin-Cre* transgenic mice [Jackson stock No. 003574] to generate *Wwox* conditional knock-out in hepatocytes (*Hep-cKO*) [25], *Adiponectine-Cre* transgenic mice [Jackson stock No. 028020] to generate *Wwox* conditional knock-out in adipose tissue (*Adipo-cKO*) [26], and *ACTA1-rtTAtetO-Cre* transgenic mice [Jackson stock No. 012433] to generate *Wwox* conditional knock-out in skeletal muscles (*SKM-cKO*) [27]. Control mice for each genotype exhibited Cre expression in *Wwox*+/+ background (Alb-Cre+;*Wwox*+/+, *Adipo-Cre*+;*Wwox*+/+, *ACTA1-etTA tetO-Cre*+;*Wwox*+/+). Male mice were weighed once every week from the age of 6 weeks up to 37 weeks. To induce *Wwox* deletion in SKM, 2 mg/mL doxycycline and 1% sucrose were added to the drinking water of both *ACTA1-rtTAtetO-Cre;Wwoxf/f* mice and *ACTA1-rtTAtetO-Cre;Wwox*+/+ control littermates in breeding cages, which were changed every 3 days and this protocol lasted until mice were euthanized for analysis. Before euthanasia, the metabolic profiles of the mice were assessed by using the Promethion High-Definition Behavioral Phenotyping System (Sable Instruments, Inc., Las Vegas, NV, USA), as described previously [28]; total body fat and lean masses were determined by EchoMRI-100H™ (Echo Medical Systems LLC, Houston, TX, USA). All experiments involving mice were approved by the Hebrew University Institutional Animal Care and Use Committee (IACUC).

4.2. MicroPET-CT scan

PET-CT scans were carried out in the Cyclotron Unit at Hadassah Medical Center according to IACUC rules. Following an overnight (12–16 h) food deprivation, mice were anesthetized with isoflurane (1%–2.5% in O_2) and maintained normothermic using a heating pad. Following a CT attenuation-correction scan, PET acquisitions were carried out in list-mode using an Inveon™ MM PET-CT small animal-dedicated scanner (Siemens Medical Solutions, USA). PET scans were initiated at the time of [^{18}F]-FDG injection via the lateral tail vein (7.8 ± 1 MBq), and lasted 1 h. Emission sinograms were normalized and corrected for attenuation, scatter, randoms, dead time, and decay. Images were reconstructed using Fourier rebinning and two-dimensional ordered-subsets expectation maximization (2D-OSEM), with a voxel size of 0.776 × 0.776 × 0.796 mm^3. Image analysis and quantification were performed using Inveon Research Workplace 4.2 (Siemens). Delineation of volumes of interest (VOIs) in the right and left gastrocnemius muscles of each animal was performed by manual segmentation, based on the corresponding CT image, and [^{18}F]-FDG time activity curves (TACs) were generated. Distribution of activity was calculated as the percentage of injected dose per mL of tissue (%ID/mL). Standardized uptake values (SUVs) were calculated as the product of %ID/mL and the total body weight of the animal.

4.3. Glucose and insulin tolerance tests (GTT and ITT)

For GTT, mice (6 months old) were fasted for 18 h, followed by an intraperitoneal (i.p.) injection of 2 g/kg body weight of glucose [52,53]. Blood glucose was measured at 0, 30, 60, 120, and 150 min. ITT was performed on 6-month-old mice after a fasting of 4 h, followed by an i.p. injection of 0.75 U/kg body weight of insulin (Biological Industries, Beit Haemek, Israel). Blood glucose was measured at 0, 30, 60, 120, and 150 min. All blood glucose measurements were carried out using an Accu-Check glucometer (Roche Diagnostics, Mannheim, Germany).

4.4. Histology of skeletal muscles

Skeletal muscles were harvested from the scarified mice, covered with OCT (Scigen Scientific Gardena, CA, USA), dipped in chilled 2-methylbutane (Isopentane) for 25 s, then transferred to frozen tissues onto dry ice for 20 min. The tissues were wrapped in aluminum foil and stored at −80 °C until sectioning. Tissues were sectioned (4 μm) in a cryostat microtome at −20 °C, and stained with hematoxylin and eosin.

4.5. Cell culture and transient transfection

C2C12 and HEK293 cells were grown in DMEM supplemented with 10% FBS (Gibco, Grand Island, USA), glutamine, and penicillin/streptomycin (Beit-Haemek, Israel). Cells were routinely authenticated, and cell aliquots from early passages were used. Transient transfections of HEK293 cells were achieved using Mirus TransLTi (Mirus Bio LLC, Wisconsin, USA) according the manufacturer's instructions. Transient transfections of C2C12 cells by WWOX siRNA (Sigma Aldrich, Germany) were achieved using lipofectamine 2000 (Thermo Fisher Scientific, CA, USA) according to the manufacturer's instructions.

4.6. Immunoprecipitation assays

Cells were lysed using NP-40 lysis buffer containing 50 mmol/L Tris (pH 7.5), 150 mmol/L NaCl, 10% glycerol, 0.5% Nonidet P-40, and protease inhibitors. Lysates were pre-cleared with mouse IgG, immunoprecipitations (IP) were carried out in the same buffer, and lysates were washed 4 times with the same buffer containing 0.1% Nonidet P-40. Antibodies used for IP were monoclonal anti-WWOX antibody [54], anti-HA (Cat # ab9110, Abcam, USA), and anti-Flag (Cat # F3165, Sigma–Aldrich, Germany).

4.7. Immunoblot analysis

For immunoblot analysis, cells were lysed using lysis buffer containing 50 mM Tris (pH 7.5), 150 mM NaCl, 10% glycerol, 0.5% Nonidet P-40, and protease inhibitors (1:100). Lysates were resolved on SDS/PAGE. Antibodies used were polyclonal anti-WWOX antibody (Cat# S2603, Epitomics, CA, USA), anti-GAPDH mouse mAB (Cat # CB 100 1, CALBIOCHEM, MA, USA), anti-HIF1α Rabbit (Cat # NB100-479, Novus Biological, CO, USA), anti-HSP90 Rabbit (Cat # CA1016, CALBIOCHEM, MA, USA), anti-pACC (Ser79) Rabbit (Cat # 3661, Cell Signaling Technology, MA, USA), anti-AMPKa Rabbit (Cat # 2532, Cell Signaling Technology, MA, USA), anti-pAMPKa (Thr 172) Rabbit (Cat # 2535, Cell Signaling Technology, MA, USA), anti-HA (Cat # ab9110, Abcam, USA), and anti-Flag (Cat # F3165, Sigma–Aldrich, Germany).

4.8. RNA extraction and real-time PCR

Total RNA was prepared using TRI reagent (Sigma Aldrich), following the manufacturer's instructions. One microgram of RNA was used for cDNA synthesis using the First-Strand cDNA Synthesis kit (Bio-Rad, Hercules, CA). Quantitative real-time PCR was performed using the Power SYBR Green PCR Master Mix (Applied Biosystems, Foster City, CA). All measurements were performed in triplicate and standardized to the levels of the *Ubc* gene. A list of primers used is provided as Supplemental Table 1.

4.9. Blood biochemistry

Serum levels of cholesterol, high-density lipoprotein (HDL), and low-density lipoprotein (LDL) were determined using the Cobas C-111 chemistry analyzer (Roche, Switzerland).

4.10. Statistics

Results of the experiments were expressed as mean ± SD or SEM. Student's t-test was used to compare the values of the test and control samples. $P < 0.05$ indicates a significant difference. * P-value <0.05, ** P-value < 0.01. Human data analysis was carried out by *Type 2 Diabetes Knowledge Portal* site (www.type2diabetesgenetics.org), which included 27 datasets in Dec. 2017.

ACKNOWLEDGMENTS

We are grateful to Ben Cohen, Daniel Steinberg, and Tirza Bidani for their technical help. The Aqeilan lab is supported by a Worldwide Cancer Research grant (grant agreement No. 14-1095) and an European Research Council (ERC)-Consolidator Grant under the European Union's Horizon 2020 research and innovation program (grant agreement No. 682118). This work was also supported in part by the Israel Science Foundation (ISF) grant (#1471/14 to J.T.).

AUTHOR CONTRIBUTIONS

Mu.A. conceived the study, performed the in vitro and in vivo experiments, and wrote the manuscript. I.K. and S.U. performed some of the in vivo experiments. Mo.A, M.P., and J.T. provided reagents, analyzed the data, and wrote the paper. R.I.A. conceived and supervised the experiments, was responsible for the overall project strategy and management, and wrote the manuscript.

CONFLICT OF INTEREST

The authors declare no competing interests.

APPENDIX A. SUPPLEMENTARY DATA

Supplementary data to this article can be found online at https://doi.org/10.1016/j.molmet.2019.01.010.

REFERENCES

[1] Kaur, J., 2014. A comprehensive review on metabolic syndrome. Cardiology Research and Practice 2014:943162.

[2] Alberti, K.G., Eckel, R.H., Grundy, S.M., Zimmet, P.Z., Cleeman, J.I., Donato, K.A., et al., 2009. Harmonizing the metabolic syndrome: a joint interim statement of the international diabetes federation task force on epidemiology and prevention; national heart, lung, and blood institute; American heart association; world heart federation; International Atherosclerosis Society; and International Association for the Study of Obesity. Circulation 120:1640–1645.

[3] DeFronzo, R.A., Gunnarsson, R., Bjorkman, O., Olsson, M., Wahren, J., 1985. Effects of insulin on peripheral and splanchnic glucose metabolism in noninsulin-dependent (type II) diabetes mellitus. Journal of Clinical Investigation 76:149–155.

[4] Malgoyre, A., Chabert, C., Tonini, J., Koulmann, N., Bigard, X., Sanchez, H., 2017. Alterations to mitochondrial fatty-acid use in skeletal muscle after chronic exposure to hypoxia depend on metabolic phenotype. Journal of Applied Physiology 122:666–674.

[5] Lynch, C.J., Xu, Y., Hajnal, A., Salzberg, A.C., Kawasawa, Y.I., 2015. RNA sequencing reveals a slow to fast muscle fiber type transition after olanzapine infusion in rats. PLoS One 10:e0123966.

[6] He, J., Watkins, S., Kelley, D.E., 2001. Skeletal muscle lipid content and oxidative enzyme activity in relation to muscle fiber type in type 2 diabetes and obesity. Diabetes 50:817–823.

[7] Nagatomo, F., Fujino, H., Kondo, H., Gu, N., Takeda, I., Ishioka, N., et al., 2011. PGC-1alpha mRNA level and oxidative capacity of the plantaris muscle in rats with metabolic syndrome, hypertension, and type 2 diabetes. Acta Histochemica et Cytochemica 44:73–80.

[8] Aqeilan, R.I., Croce, C.M., 2007. WWOX in biological control and tumorigenesis. Journal of Cellular Physiology 212:307–310.

[9] Chang, N.S., Hsu, L.J., Lin, Y.S., Lai, F.J., Sheu, H.M., 2007. WW domain-containing oxidoreductase: a candidate tumor suppressor. Trends in Molecular Medicine 13:12–22.

[10] Del Mare, S., Salah, Z., Aqeilan, R.I., 2009. WWOX: its genomics, partners, and functions. Journal of Cellular Biochemistry 108:737–745.

[11] Aqeilan, R.I., Abu-Remaileh, M., Abu-Odeh, M., 2014. The common fragile site FRA16D gene product WWOX: roles in tumor suppression and genomic stability. Cellular and Molecular Life Sciences: CMLS 71:4589–4599.

[12] Dayan, S., O'Keefe, L.V., Choo, A., Richards, R.I., 2013. Common chromosomal fragile site FRA16D tumor suppressor WWOX gene expression and metabolic reprograming in cells. Genes Chromosomes & Cancer 52:823–831.

[13] Iatan, I., Choi, H.Y., Ruel, I., Reddy, M.V., Kil, H., Lee, J., et al., 2014. The WWOX gene modulates high-density lipoprotein and lipid metabolism. Circulation Cardiovascular Genetics 7:491–504.

[14] O'Keefe, L.V., Colella, A., Dayan, S., Chen, Q., Choo, A., Jacob, R., et al., 2011. Drosophila orthologue of WWOX, the chromosomal fragile site FRA16D tumour suppressor gene, functions in aerobic metabolism and regulates reactive oxygen species. Human Molecular Genetics 20:497–509.

[15] Abu-Remaileh, M., Aqeilan, R.I., 2014. Tumor suppressor WWOX regulates glucose metabolism via HIF1alpha modulation. Cell Death & Differentiation.

[16] Abu-Remaileh, M., Seewaldt, V.L., Aqeilan, R.I., 2014. WWOX loss inactivates aerobic glycolysis. Molecular and Cellular Oncology 2.

[17] Aqeilan, R.I., Hassan, M.Q., de Bruin, A., Hagan, J.P., Volinia, S., Palumbo, T., et al., 2008. The WWOX tumor suppressor is essential for postnatal survival and normal bone metabolism. Journal of Biological Chemistry 283:21629–21639.

[18] Abdeen, S.K., Del Mare, S., Hussain, S., Abu-Remaileh, M., Salah, Z., Hagan, J., et al., 2013. Conditional inactivation of the mouse Wwox tumor suppressor gene recapitulates the null phenotype. Journal of Cellular Physiology 228:1377–1382.

[19] Abdeen, S.K., Ben-David, U., Shweiki, A., Maly, B., Aqeilan, R.I., 2018. Somatic loss of WWOX is associated with TP53 perturbation in basal-like breast cancer. Cell Death & Disease 9:832.

[20] Abu-Remaileh, M., Khalaileh, A., Pikarsky, E., Aqeilan, R.I., 2018. WWOX controls hepatic HIF1alpha to suppress hepatocyte proliferation and neoplasia. Cell Death & Disease 9:511.

[21] Wang, K., Li, W.D., Zhang, C.K., Wang, Z., Glessner, J.T., Grant, S.F., et al., 2011. A genome-wide association study on obesity and obesity-related traits. PLoS One 6:e18939.

[22] Nizamuddin, S., Govindaraj, P., Saxena, S., Kashyap, M., Mishra, A., Singh, S., et al., 2015. A novel gene THSD7A is associated with obesity. International Journal of Obesity (London) 39:1662–1665.

[23] Tsai, F.J., Yang, C.F., Chen, C.C., Chuang, L.M., Lu, C.H., Chang, C.T., et al., 2010. A genome-wide association study identifies susceptibility variants for type 2 diabetes in Han Chinese. PLoS Genetics 6:e1000847.

[24] Cho, Y.S., Chen, C.H., Hu, C., Long, J., Ong, R.T., Sim, X., et al., 2011. Meta-analysis of genome-wide association studies identifies eight new loci for type 2 diabetes in east Asians. Nature Genetics 44:67–72.

[25] Postic, C., Shiota, M., Niswender, K.D., Jetton, T.L., Chen, Y., Moates, J.M., et al., 1999. Dual roles for glucokinase in glucose homeostasis as determined by liver and pancreatic beta cell-specific gene knock-outs using Cre recombinase. Journal of Biological Chemistry 274:305–315.

[26] Eguchi, J., Wang, X., Yu, S., Kershaw, E.E., Chiu, P.C., Dushay, J., et al., 2011. Transcriptional control of adipose lipid handling by IRF4. Cell Metabolism 13:249–259.

[27] Rao, P., Monks, D.A., 2009. A tetracycline-inducible and skeletal muscle-specific Cre recombinase transgenic mouse. Developments of Neurobiology 69:401–406.

[28] Udi, S., Hinden, L., Earley, B., Drori, A., Reuveni, N., Hadar, R., et al., 2017. Proximal tubular cannabinoid-1 receptor regulates obesity-induced CKD. Journal of the American Society of Nephrology 28:3518–3532.
[29] Reyes, N.L., Banks, G.B., Tsang, M., Margineantu, D., Gu, H., Djukovic, D., et al., 2015. Fnip1 regulates skeletal muscle fiber type specification, fatigue resistance, and susceptibility to muscular dystrophy. Proceedings of the National Academy of Sciences of the United States of America 112:424–429.
[30] Ruderman, N.B., Carling, D., Prentki, M., Cacicedo, J.M., 2013. AMPK, insulin resistance, and the metabolic syndrome. Journal of Clinical Investigation 123: 2764–2772.
[31] Cokorinos, E.C., Delmore, J., Reyes, A.R., Albuquerque, B., Kjobsted, R., Jorgensen, N.O., et al., 2017. Activation of skeletal muscle AMPK promotes glucose disposal and glucose lowering in non-human primates and mice. Cell Metabolism 25:1147–1159 e1110.
[32] Abu-Odeh, M., Bar-Mag, T., Huang, H., Kim, T., Salah, Z., Abdeen, S.K., et al., 2014. Characterizing WW domain interactions of tumor suppressor WWOX reveals its association with multiprotein networks. The Journal of Biological Chemistry 289:8865–8880.
[33] DeFronzo, R.A., Tripathy, D., 2009. Skeletal muscle insulin resistance is the primary defect in type 2 diabetes. Diabetes Care 32(Suppl 2):S157–S163.
[34] Civitarese, A.E., MacLean, P.S., Carling, S., Kerr-Bayles, L., McMillan, R.P., Pierce, A., et al., 2010. Regulation of skeletal muscle oxidative capacity and insulin signaling by the mitochondrial rhomboid protease PARL. Cell Metabolism 11:412–426.
[35] Nakaya, Y., Ohnaka, M., Sakamoto, S., Niwa, Y., Okada, K., Nomura, M., et al., 1998. Respiratory quotient in patients with non-insulin-dependent diabetes mellitus treated with insulin and oral hypoglycemic agents. Annals of Nutrition & Metabolism 42:333–340.
[36] Kelley, D.E., He, J., Menshikova, E.V., Ritov, V.B., 2002. Dysfunction of mitochondria in human skeletal muscle in type 2 diabetes. Diabetes 51: 2944–2950.
[37] Wang, M., Wang, X.C., Zhang, Z.Y., Mou, B., Hu, R.M., 2010. Impaired mitochondrial oxidative phosphorylation in multiple insulin-sensitive tissues of humans with type 2 diabetes mellitus. Journal of International Medical Research 38:769–781.
[38] Crawford, S.O., Hoogeveen, R.C., Brancati, F.L., Astor, B.C., Ballantyne, C.M., Schmidt, M.I., et al., 2010. Association of blood lactate with type 2 diabetes: the atherosclerosis risk in communities carotid MRI study. International Journal of Epidemiology 39:1647–1655.
[39] Kleinridders, A., Ferris, H.A., Cai, W., Kahn, C.R., 2014. Insulin action in brain regulates systemic metabolism and brain function. Diabetes 63:2232–2243.
[40] Kersten, S., 2001. Mechanisms of nutritional and hormonal regulation of lipogenesis. EMBO Reports 2:282–286.
[41] Semenza, G.L., 2011. Hypoxia-inducible factor 1: regulator of mitochondrial metabolism and mediator of ischemic preconditioning. Biochimica et Biophysica Acta 1813:1263–1268.
[42] Sutendra, G., Dromparis, P., Kinnaird, A., Stenson, T.H., Haromy, A., Parker, J.M., et al., 2013. Mitochondrial activation by inhibition of PDKII suppresses HIF1a signaling and angiogenesis in cancer. Oncogene 32:1638–1650.
[43] Hardie, D.G., Ross, F.A., Hawley, S.A., 2012. AMPK: a nutrient and energy sensor that maintains energy homeostasis *Nature reviews*. Molecular Cell Biology 13:251–262.
[44] Mihaylova, M.M., Shaw, R.J., 2011. The AMPK signalling pathway coordinates cell growth, autophagy and metabolism. Nature Cell Biology 13:1016–1023.
[45] Lee, W.J., Kim, M., Park, H.S., Kim, H.S., Jeon, M.J., Oh, K.S., et al., 2006. AMPK activation increases fatty acid oxidation in skeletal muscle by activating PPARalpha and PGC-1. Biochemical and Biophysical Research Communications 340:291–295.
[46] Glund, S., Schoelch, C., Thomas, L., Niessen, H.G., Stiller, D., Roth, G.J., et al., 2012. Inhibition of acetyl-CoA carboxylase 2 enhances skeletal muscle fatty acid oxidation and improves whole-body glucose homeostasis in db/db mice. Diabetologia 55:2044–2053.
[47] Lantier, L., Fentz, J., Mounier, R., Leclerc, J., Treebak, J.T., Pehmoller, C., et al., 2014. AMPK controls exercise endurance, mitochondrial oxidative capacity, and skeletal muscle integrity. The FASEB Journal 28:3211–3224.
[48] O'Neill, H.M., Lally, J.S., Galic, S., Thomas, M., Azizi, P.D., Fullerton, M.D., et al., 2014. AMPK phosphorylation of ACC2 is required for skeletal muscle fatty acid oxidation and insulin sensitivity in mice. Diabetologia 57:1693–1702.
[49] Amoasii, L., Holland, W., Sanchez-Ortiz, E., Baskin, K.K., Pearson, M., Burgess, S.C., et al., 2016. A MED13-dependent skeletal muscle gene program controls systemic glucose homeostasis and hepatic metabolism. Genes & Development 30:434–446.
[50] Lee, M., Hwang, J.T., Lee, H.J., Jung, S.N., Kang, I., Chi, S.G., et al., 2003. AMP-activated protein kinase activity is critical for hypoxia-inducible factor-1 transcriptional activity and its target gene expression under hypoxic conditions in DU145 cells. Journal of Biological Chemistry 278:39653–39661.
[51] Thomas, A., Belaidi, E., Moulin, S., Horman, S., van der Zon, G.C., Viollet, B., et al., 2017. Chronic intermittent hypoxia impairs insulin sensitivity but improves whole-body glucose tolerance by activating skeletal muscle AMPK. Diabetes 66:2942–2951.
[52] Xu, X., Pang, J., Chen, Y., Bucala, R., Zhang, Y., Ren, J., 2016. Macrophage migration inhibitory factor (MIF) deficiency exacerbates aging-induced cardiac remodeling and dysfunction despite improved inflammation: role of autophagy regulation. Scientific Reports 6:22488.
[53] Sun, Y., Asnicar, M., Saha, P.K., Chan, L., Smith, R.G., 2006. Ablation of ghrelin improves the diabetic but not obese phenotype of ob/ob mice. Cell Metabolism 3:379–386.
[54] Aqeilan, R.I., Pekarsky, Y., Herrero, J.J., Palamarchuk, A., Letofsky, J., Druck, T., et al., 2004. Functional association between Wwox tumor suppressor protein and p73, a p53 homolog. Proceedings of the National Academy of Sciences of the United States of America 101:4401–4406.

